Yield stress thixotropic clay suspension: Investigations of structure by light, neutron, and x-ray scattering

Frédéric Pignon,[1] Albert Magnin,[1] Jean-Michel Piau,[1] Bernard Cabane,[2] Peter Lindner,[3] and Olivier Diat[4]
[1]*Laboratoire de Rhéologie, Université Joseph Fourier, Grenoble I, Institut National Polytechnique de Grenoble, CNRS UMR No. 5520, Boîte Postale 53, 38041 Grenoble Cedex 9, France*
[2]*Equipe Mixte CEA-RP, Rhône-Poulenc, 93308 Aubervilliers, France*
[3]*Institut Laue-Langevin, Boîte Postale 156, F-38042 Grenoble Cedex 9, France*
[4]*ESRF, Boîte Postale 220, F-38043 Grenoble, France*
(Received 5 December 1996; revised manuscript received 29 May 1997)

The characteristic length scales of the structure and fractal behavior of a thixotropic colloidal suspension of synthetic clay were studied by using a combination of small-angle neutron and x-ray scattering and static light scattering. At the same time, macroscopic mechanical behavior at rest was characterized by means of rheometric measurements. Two characteristic length scales were detected in these yield stress suspensions of discotic texture. The first, measuring several tens of nanometres, is linked to a fractal dimension of 3. The second, of the order of 1 μm, is linked to a fractal behavior of dimension D that increases with the particle volume fraction. Consequently, it is suggested that the structure of the dispersions at rest is composed of subunits measuring a few tens of nanometers that combine to form dense aggregates measuring about 1 μm. At larger length scales, these micrometer-sized aggregates are rearranged to form a continuous three-dimensional isotropic structure that has a fractal behavior of dimension D, which gives the gels their texture. The increase of this fractal dimension with the particle volume fraction, the ionic strength, and the gelation time is correlated to a hardening of the mechanical properties of the gels at rest. The gel state is reached above a volume fraction ϕ_v^* for a given ionic strength and gelation time. In the gel phase, a critical volume fraction ϕ_{vc} separates two domains. Gels belonging to the domain $\phi_v^* < \phi_v < \phi_{vc}$ have a fractal behavior of dimension $D = 1 \pm 0.05$, suggesting an alignment of the micrometer-sized aggregates that leads to the formation of a mechanically weak fibrous structure. Gels belonging $\phi_v > \phi_{vc}$ have a fractal dimension $D = 1.8 \pm 0.01$, corresponding to a mechanically stronger structure consisting of zones of high and lower particle density. A scaling law enabled these fractal dimensions to be correlated with the effect of the volume fraction on the yield stress. In contrast to what is commonly assumed in relation to clay suspensions, it is suggested here that it is the large length scales, of the order of 1 μm, associated with a fractal arrangement that governs the macroscopic mechanical behavior. [S1063-651X(97)07209-7]

PACS number(s): 82.70.Kj, 83.70.Hq

I. INTRODUCTION

The suspension studied here was made with Laponite, a synthetic clay of the hectorite type. In an aqueous medium, this forms a transparent thixotropic gel above a certain volume fraction, at a low ionic strength of $I_s \leqslant \times 10^{-3} M$ and pH of 9.5. The clay consists of discotic particles of uniform size, about 300 Å in diameter and about 20 Å in thickness [1].

Owing to its high purity and very small crystal size, this is perfectly suited to light-scattering measurements as, unlike natural clays at the same concentration, it does not produce any multiple scattering. In addition, it has macroscopic volume properties (yield stress and thixotropy) that need to be linked with the mesoscopic properties of the system, i.e., its structure, in order to be better understood and controlled.

Many structural models relating to this clay suspension already have been proposed by different authors in order to try to explain the mechanism of swelling gel in time and its thixotropic behavior. Certain authors have described the formation of a so-called ''house of cards'' network, where electrostatic attraction appears to occur between the edges of the positively charged platelets and the negatively charged faces [2,3]. Others have demonstrated the existence in the suspending medium of tactoids, i.e., piles of two to four individual platelets separated by a few layers of water [4,5]. Ramsay and Lindner [6] concluded from small-angle neutron-scattering measurements that the formation of a balanced gel structure is due essentially to repulsion between the isolated microcrystals of clay. They detected short-range correlations and alignments between the particles in a structure that is isotropic over longer ranges. Morvan *et al.* [7] have shown a Q^{-3} power-law decay by ultrasmall and small-angle x-ray scattering (SAXS), in a region of modulus of scattering vectors of about 1×10^{-3} Å^{-1}. This power-law decay is attributed to a large-scale organization, i.e., a variably dense network and a heterogeneous structure. They proposed two possible microstructures: (i) an edge-face contact leading to a card-house structure and (ii) a locally parallel interaction between first neighbors due to osmotic repulsion between adjacent platelets. Most recently, Mourchid *et al.* [8] have studied the structure and sol-gel transition of these Laponite suspensions by means of cryofracture, TEM, SAXS, and rheometric measurements. They have put forth a hypothesis that tallies with their own observations and may explain the sol-gel transition. This hypothesis considers the

existence of oriented microdomains, consisting of particles in the form of platelets. These oriented microdomains of grouped particles should develop as ionic strength increases, leading to the formation of large regions with lower particle densities. The interconnection and/or interrelation of these microdomains is, according to them, responsible for the appearance of the gel phase.

The previous studies revealed, on the one hand, the existence and nature of the interactions occurring between the suspended particles and, on the other hand, the structural schemes. However, as far as the present authors are aware, no pertinent length scale has been proposed for the structure in suspensions of Laponite. The purpose of this article is to identify these characteristic length scales and to relate them to the macroscopic behaviors observed in these thixotropic suspensions.

The method used to study the structure and interparticle interactions within this colloidal clay suspension was that of angular scattering of different types of radiation. At the same time, the nature of the various flow regimes within the suspension was determined by means of rheometric measurements associated with visualization of the strain field [9].

Angular radiation scattering measurements were taken so as to cover as wide a scattering vector domain as possible, with a view to obtaining structural information ranging from the size of the particle (a few nanometers) to the scale of the largest structures (a few micrometers). The modulus of the scattering vector is defined by $Q=(4\pi n/\lambda)\sin(\theta/2)$, where n is the refractive index of the suspending medium (in the case of light-scattering measurements), λ the wavelength of the radiation, and θ the scattering angle. The small-angle neutron and x-ray scattering measurements overlap, making it possible to cover a Q domain ranging from 1×10^{-3} to 1×10^{-1} Å^{-1}. The light-scattering measurements cover a Q domain ranging from 2×10^{-5} to 4×10^{-4} Å^{-1}. This means that it is possible to investigate all the long-range interactions between particles and to extend the scattering intensity behavior as a function of the modulus of the scattering vector, observed by neutron and x-ray scattering.

Owing to the size of the Q domain explored by both neutron and light scattering, it is possible to demonstrate the existence of two length scales that are characteristic of the structure of the suspension and to determine the nature of the interparticle interactions occurring within it. By determining the influence of the volume fraction on the yield stress value, it was possible to define a scaling law related to the fractal dimension of the suspending objects. The influence of the ionic strength on the equilibrium structure showed that the fractal dimension is a decisive parameter of the macroscopic behavior.

II. MATERIALS AND METHODS

A. Materials

The synthetic clay used for the experiments is Laponite XLG, manufactured by Laporte Industry. The chemical composition of the clay is as follows: 66.2% of SiO_2, 30.2% of MgO, 2.9% of Na_2O, and 0.7% of Li_2O, which corresponds to the chemical formula [6]

$$Si_8[Mg_{5.5}Li_{0.4}H_{4.0}O_{24.0}]^{0.7-}Na_{0.7}^{0.7+}.$$

The suspension is prepared as follows. The clay powder is mixed in a solution of distilled water and NaCl at different concentrations. This is then stirred for 30 min at a temperature of about 20 °C, by means of a deflocculating vane rotating at 1500 rpm. A few hours after stirring, a transparent gel is formed, with a ionic strength denoted I_s.

Interparticle interactions take place as the clay swells following preparation. The suspended particles are thus subject to electrostatic repulsion and attraction, which are in competition with the van der Waals attraction, polar repulsion between water molecules adsorbed at the surface, interparticle excluded-volume effects, and Brownian motion. Depending on the particle concentration, the ion content of the water, and the pH value, these interactions may give rise to a stable colloidal solution, an elastic gel, plastic paste, or even separate solid and liquid phases [8].

The pH value of all the preparations studied in this article was adjusted to 9.5 in order to avoid any consecutive dissolution of the material. Indeed, Thomson and Butterworth [10] showed that there is significant dissolution of magnesium silicate with pH values of less than 7 and the disappearance of such dissolution at pH values above 9.

The study domain corresponds to that in which a thixotropic gel is obtained above the volume fraction ϕ_v^* defining the sol-gel transition. With a weak ionic strength ($I_s=1\times10^{-3}M$), at a pH of 9.5, this domain extends in concentration from 0.9×10^{-2} to 5×10^{-2} g ml^{-1}, corresponding to a volume fraction ϕ_v of 0.35–2 %. The density of the particles is 2.53 g cm^{-3} [5].

Changes were observed in the viscoelastic properties and fractal dimensions of the present system over periods of several months. This temporal instability is probably due, on the one hand, to osmotic swelling caused by repulsion between the double layers and, on the other hand, to the progressive organization of the particles in fractal aggregates over increasing distances. The aggregation process was followed at the largest length scales by static light scattering in order to quantify this temporal instability.

B. Small-angle x-ray scattering

The measurements were made at the European Synchrotron Radiation Facility in Grenoble, on the ''High Brilliance Beamline'' [11]. The photon wavelength was 0.95 Å and the gas-filled detector was placed between 2 and 7 m from the sample position in order to cover a Q domain between 6×10^{-3} and 1×10^{-1} Å^{-1}. Samples were placed in a Couette shear cell, designed for x-ray experiments [12]. The sample gap between both cylinders (rotor and stator with 0.5 mm thickness of polycarbonate material) was 1 mm. The scattering from the empty cell limited the smallest-Q values that could really be achieved. Conventional integration programs were used to obtain the radial mean of the scattering intensity.

C. Small-angle neutron scattering

The measurements were made at the Institute Laue-Langevin in Grenoble, using the D11 instrument, with a wavelength of 6 Å. The samples were placed at distances of 2.5, 10, and 35.7 m from the two-dimensional detector, with beam collimations of, respectively, 2.5, 20.5, and 40.5 m.

The static measurements were obtained by placing the samples in the Couette shear cell developed by Lindner and Oberthür [13]. This quartz cell consists of a fixed inner cylinder (stator) and a rotating outer cylinder (rotor). The stator is 46 mm in diameter and the gap is 0.5 mm wide, so that the sample crossed by radiation is 1 mm thick in total. We plan to discuss the results relating to shear in the future. The detector consists of a set of 64×64 elements measuring $1\times1\ \mathrm{cm}^2$. The data were analyzed using standard programs in order to remove any background inconsistencies. The mean was then taken radially over the total intensity of scattering, using classic integration software.

D. Static light scattering

The laser test facility used for the experiment was developed and built at the Laboratoire de Rhéologie in Grenoble [14]. It consists of a 2-mW laser beam (He-Ne) with a wavelength of 6328 Å and a Fresnel lens acting as scattering screen. The detector is a video camera with a charge coupled device 752×582 pixel sensor. A shutter enables acquisition time to be varied between $\frac{1}{50}$ and $\frac{1}{10\,000}$ s. Image processing is used for the analysis and the conventional integration operations are carried out by a specific software. The samples were placed in a plate-plate shear cell composed of two parallel rectangular strips of glass. The results relating to shear will be discussed in the future. The thickness of the sample is fixed at 0.30 mm and transmission measurements give satisfactory results for these small thicknesses ($I_{\mathrm{transmitted}}/I_{\mathrm{incident}}\approx0.95$). When the sample is placed in the measurement cell, it may be subjected to mechanical stresses and partial breakdown of its structure. For this reason, it is left to rest in the cell for 10 min before any measurements are made. Successive checks were carried out at different periods after the sample had been installed in order to make sure that 10 min was a sufficient time for the light-scattering results as a function of Q not to be affected by any possible structure breakdown. Experimental data scatter over fractal dimensions D is 5%, taking into account several measurements at all volume fractions.

E. Rheometric techniques

The tests were carried out at a temperature of 20 °C (±1 °C). Yield stress measurements were carried out using the vane method on a Weissenberg-Carrimed controlled speed rheometer. These enabled the change in yield stress to be defined as a function of volume fraction [15]. A cone-plate configuration of radius $r=24.5$ mm and angle $\alpha=0.076$ rad was chosen for dynamic shear. Torsion bar torque sensors were used. In order to avoid interfacial effects, the surfaces of the apparatus were covered with glass paper of 200-μm roughness, except around the central part. To avoid evaporation from the sample during the test, the atmosphere around it was saturated with water [9–16].

In order to characterize the viscoelastic properties of these thixotropic clay suspensions, one of the procedures described in Ref. [9] was used. This involves breaking down the structure of the sample as it is crushed between the cone and plate and monitoring the way in which its structure reforms by measuring the viscoelastic moduli G' and G'' in time (Fig. 1). In order to define the viscoelastic linear domain in these

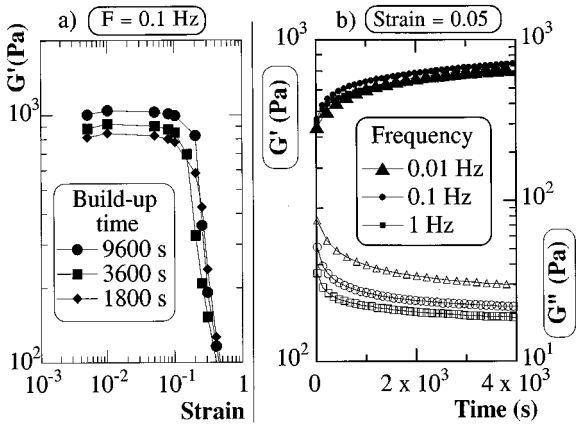

FIG. 1. Determination of the viscoelastic linear domain in a harmonic shear test on a Laponite suspension at a volume fraction of 1.2%, $I_s=1\times10^{-3}M$, $p\mathrm{H}=9.5$, and $t_p=445$ days. (a) Changes in elastic modulus as a function of the strain applied to the sample at various structural recovery times after crushing in the cone-plate apparatus. (b) Changes in viscoelastic moduli as a function of the frequency of shear during structural recovery after crushing in the cone-plate apparatus.

materials with time-dependent rheological properties, it is necessary to take into account the state of structural recovery of the sample. To do this, two types of test were performed to evaluate the extent of the viscoelastic linear domain for various ranges of frequency and strain.

In the first test, at a fixed frequency of $F=0.1$ Hz and at various structural recovery times, the sample was subjected to a strain sweep of 0.005–0.3 for a period of 600 s [Fig. 1(a)]. The extent of the viscoelastic linear domain from 0.005 to 0.1 is slightly influenced by the state of structural recovery of the material. Furthermore, the elastic modulus levels reached increase with structural recovery time. This linear strain domain is therefore valid for recovery times of at least 1800 s, for which the kinetics of recovery are slow.

In the second test, with a fixed strain amplitude ($\gamma=0.05$) corresponding to the linear strain domain described above, the structural recovery of the sample after crushing is monitored for various oscillation frequency values. This second test [Fig. 1(b)] shows that within the range of error of the experiments ($\pm10\%$), the response of the viscoelastic moduli in time is independent of the frequency and a linear viscoelastic domain can thus be defined, running from 0.01 to 1 Hz for $\gamma=0.05$.

These two tests show that the viscoelastic linear domain ($0.005\leqslant\gamma\leqslant0.1$ and $0.01\leqslant F\leqslant1$) is independent of the structural recovery time for times of at least 1800 s after crushing in the cone-plate assembly. As the purpose here is to study the state of the structure after recovery and not to monitor the actual recovery process, a strain of 0.05 and frequency of 0.1 Hz will be chosen in the remainder of this article and the viscoelastic measurements will be compared only for recovery times of more than 1800 s.

Furthermore, oscillatory shear experiments were performed by Willenbacher [17], on Laponite dispersions, at different volume fractions of between 0.48% and 1.2%, prepared using NaCl solutions of various ionic strengths ($0.0017M$ and $0.052M$). He showed that the linear viscoelas-

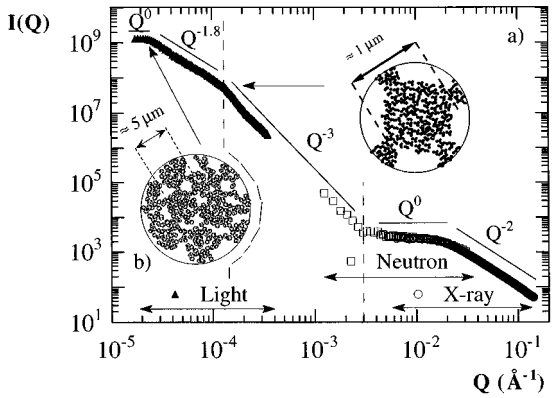

FIG. 2. Small-angle x-ray and neutron scattering and static light scattering from an aqueous Laponite suspension at rest, at volume fraction 1.6%, $I_s = 1\times10^{-3}M$, pH = 9.5, and $t_p = 200$ days. (a) Dense micrometer-sized aggregates and (b) mass fractal made of alternating aggregates and voids.

tic regime extended for strain amplitudes from 0.001 to 0.1. He was able to establish that the storage modulus G' dominates G'' by more than one order of magnitude and is essentially independent of frequency in the entire frequency domain investigated from 1.6×10^{-3} to 6 Hz. For these data the sample was allowed to rest for 15 min before the measurement was started.

III. RESULTS AND DISCUSSION

A. Physical structure of the gel

An overall view of the structure and interactions may be obtained from the complete scattering curve $I(Q)$ of the Laponite gel made at a volume fraction 1.6%, NaCl concentration $I_s = 10^{-3}M$, and pH 9.5 (Fig. 2). This scattering curve was obtained by combining the data from SAXS, small-angle neutron scattering (SANS), and static light scattering in such a way that the magnitudes of the slopes of the three sets of data matched each other in a log-log plot. This scattering curve is analyzed according to the ranges of Q values, starting from the highest (1×10^{-1} Å^{-1}), which correspond to intraparticle dimensions (a few nanometers), and ending with the lowest (2×10^{-5} Å^{-1}), which correspond to the large-scale organization of the gel (5 μm).

At high-Q values, between 1×10^{-1} and 3×10^{-2} Å^{-1}, the scattered intensity follows a Q^{-2} power-law decay (Fig. 2). This decay is consistent with the scattering expected from platelets with random orientations.

Between 1.5×10^{-2} and 3×10^{-3} Å^{-1}, there is a plateau of the intensity. As will be shown below, this plateau is more extended at higher particle concentrations and vanishes at low particle concentrations. Ramsay and Lindner [6] have shown that this plateau turns into a peak at still higher particle concentrations. Therefore, it is produced by interparticle interferences. The depression of the intensity in this range means that density fluctuations are suppressed, i.e., that the number density of particles is homogeneous over length scales that are between 70 and 350 Å.

Between 3×10^{-3} and 1×10^{-3} Å^{-1}, the SANS intensities are above the plateau and follow a Q^{-3} power law. If the platelets were uniformly dispersed in the gel, then the intensity would be flat in this range. Therefore, the excess scattered intensity above the plateau value must be produced by spatial variations in the concentration of platelets, i.e., dense regions (''micro-domains'') separated by less dense regions (''voids''). This excess scattering and the Q^{-3} power law already have been observed by Morvan *et al.* [7] on a Laponite gel at volume fraction 4.2% and low ionic strength and then by Mourchid *et al.* [8] on Laponite gels at volume fractions 1.5% and 5.2% and high ionic strength. According to these authors, the high ionic strength promotes the formation of such microdomains. The Q^{-3} power law indicates that the dimensions of these microdomains range from a smallest size, which is $a = 1/(3\times10^{-3}\ \text{Å}^{-1}) \approx 350$ Å, to a largest size L, which is about 1 μm, as will be seen below.

The light-scattering measurements reveal two successive types of fractal organization, separated by the characteristic dimension L. In the scattering curve, the first type of fractal behavior corresponds to a continuation of the Q^{-3} power law observed in SANS. It is observed over a range of Q values extending from $Q = 3\times10^{-3}$ to 1.2×10^{-4} Å^{-1}. The Q^{-3} slope implies that the gel structure is self-similar over distances ranging from $a = 350$ Å to $L = 1$ μm. The exponent -3 can be interpreted in different ways.

(i) The objects that cause the scattering are dense aggregates of subunits of size a. Their interior is homogeneous, but their surface is fractal. The scale of surface roughness is $a = 350$ Å. The overall size of the objects is 1 μm.

(ii) This way is similar to (i), but there is a size distribution of the aggregates: the smallest have size a and the largest have size L. The exponent -3 no longer reflects the surface roughness of the aggregates, but their size distribution.

In both interpretations, a two-step aggregation process is required: First the particles associate to form subunits of size $a = 350$ Å and then the subunits associate to form larger, dense aggregates with rough surfaces or a broad size distribution. A similar aggregation behavior has been observed also by Axford and Herrington [18] in suspensions of natural Bentonite clay.

The second type of fractal organization is characterized by a $Q^{-1.8}$ power law, observed from $Q = 1.2\times10^{-4}$ to 2×10^{-5} Å^{-1}. Accordingly, there is a range of distances, ranging from $L = 1$ μm to $\xi = 5$ μm, where the gel structure is again self-similar. The exponent -1.8 implies that the organization is a mass fractal, i.e., made of an alternation of aggregates and voids. Moreover, the exponent -1.8 is that expected for aggregation resulting from cluster-cluster aggregation [19–21]. Accordingly, the dense aggregates observed at dimensions below L are themselves more loosely aggregated up to sizes of the order of $\xi = 5$ μm.

Finally, at Q values below 2×10^{-5} Å^{-1}, the scattering curve becomes flat, indicating that there are no heterogeneities of sizes larger than $\xi = 5$ μm. Thus the gel structure is homogeneous at larger scales.

The most likely type of structure that matches these results is represented schematically in Fig. 3. It consists of small clusters of size $a = 350$ Å (the subunits), each containing a few platelets, which are combined to form dense aggregates of sizes $L = 1$ μm. These micrometer-sized aggregates are loosely interconnected to form a continuous, isotropic network that forms the texture of the gel.

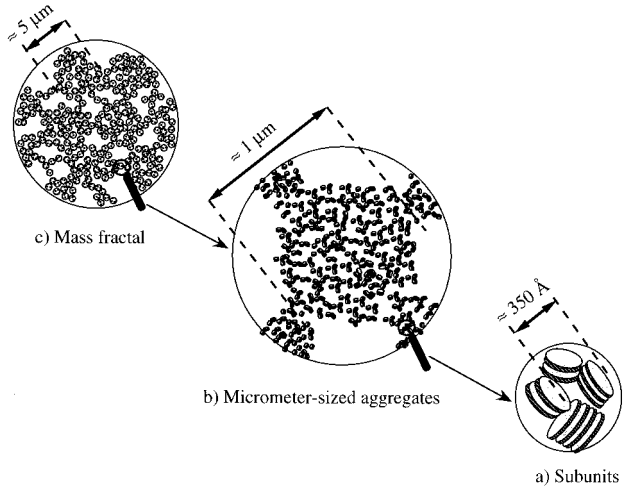

FIG. 3. Schematic representation of structure of Laponite suspension at rest. The network is made of two types of characteristic aggregates: (a) subunits of oriented clay particles, which define the first length scale of about a few nanometers, and (b) aggregates of tight isotropic distributions of subunits, which define the second length scale of about 1 μm. (c) The loose connection of these micrometer-sized aggregates gives rise to an isotropic equilibrium structure.

B. Interparticle correlations

The scattering curves shown in Fig. 2 result from interferences between pairs of scatters in the sample. These interferences are of two types: interferences of pairs that belong the same particle (intraparticle) and interferences of pairs that belong to distinct particles (interparticle). At low concentrations and at short distances (high Q), intraparticle interferences are dominant. At high concentrations and at long distances (low Q), interparticle interferences are dominant. The effect of concentration is clearly visible on the part of the scattering curves that corresponds to distances between neighboring particles, i.e., between 1.5×10^{-3} and 1.5×10^{-2} Å^{-1} (Fig. 4): In this range, the ''plateau'' of the scattering curves is a signature of interparticle interferences.

In order to extract the organization of the particles from the scattering curves, it is necessary to separate these two

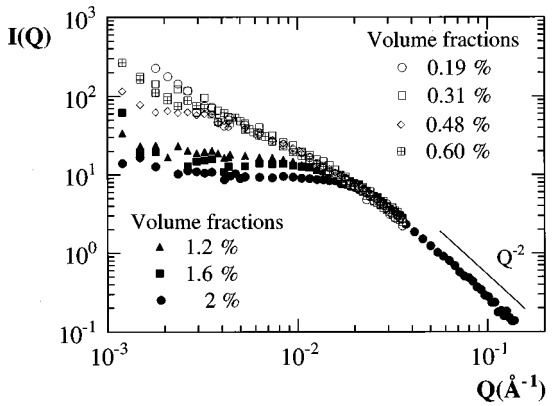

FIG. 4. SANS from Laponite suspensions at rest, at different volume fractions. With increasing volume fractions, a short-range order develops inside aggregates of about a few nanometers. $I_s=1\times10^{-3}M$, pH$=9.5$, and $t_p=380$ days.

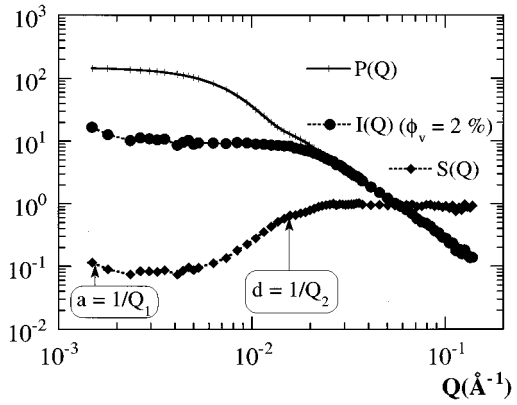

FIG. 5. Form factor $P(Q)$, scattering intensity $I(Q)$, and structure factor $S(Q)$ for Laponite suspensions at 2% volume fraction, $I_s=1\times10^{-3}M$, pH$=9.5$, and $t_p=380$ days.

types of interferences. This can be done in two steps. (a) Calculate a single-particle scattering function $P(Q)$ on the basis of a postulated model for the particle shape [22]. (b) Assume that the scattered intensity can be expressed as

$$I(Q)=NP(Q)S(Q), \tag{1}$$

where N is the number density of particles, $P(Q)$ the single-particle scattering function, and $S(Q)$ the structure factor of the dispersion that describes pair correlations between particles. This assumption holds as long as there is no correlation between the relative locations of particles and their respective orientations.

We assume that the particle are disks, with a thickness $2H_p$ and a radius R_p. If they take random orientations, the single-particle scattering function may be calculated as an average over all orientations

$$P(Q)=\int_0^{\pi/2}\frac{\sin^2(QH_p\cos\alpha_p)4J_1^2(QR_p\sin\alpha_p)}{(QH_p\cos\alpha_p)^2(QR_p\sin\alpha_p)^2}\times\sin(\alpha_p)d\alpha_p, \tag{2}$$

where α_p is the angle between the axis of the disk and the scattering vector and J_1 is the first-order Bessel function. We choose $R_p=300$ Å and $2H_p=10$ Å. With this choice, the calculated function $P(Q)$ reproduces the high part of the measured scattering curves (Fig. 5). At lower-Q values, below 1.5×10^{-2} Å^{-1}, the data are below the calculated $P(Q)$ curve. According to Eq. (1), this depression is caused by interparticle interferences.

The corresponding structure factor $S(Q)$ is also shown in Fig. 5. At high-Q values, beyond 1.5×10^{-2} Å^{-1}, $S(Q)$ is close to unity. This was expected, since interferences at distances below 70 Å are predominantly intraparticle. At lower-Q values, between 1.5×10^{-3} and 1.5×10^{-2} Å^{-1}, there is a strong depression of $S(Q)$. As shown by Mourchid *et al.* [8], this depression originates from interparticle repulsions that eliminate fluctuations particles concentration in the range 70–700 Å.

At higher concentrations, the depression of $S(Q)$ is deeper and broader (Fig. 6). The extent of this depression gives a measure of how far concentration fluctuations are

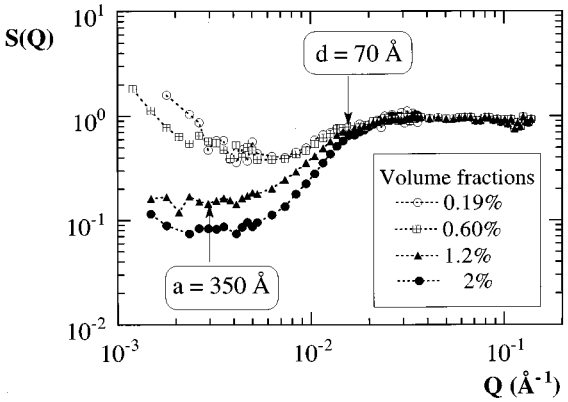

FIG. 6. Structure factor $S(Q)$ for Laponite suspensions at different volume fractions, $I_s=1\times10^{-3}M$, pH=9.5, and t_p =380 days.

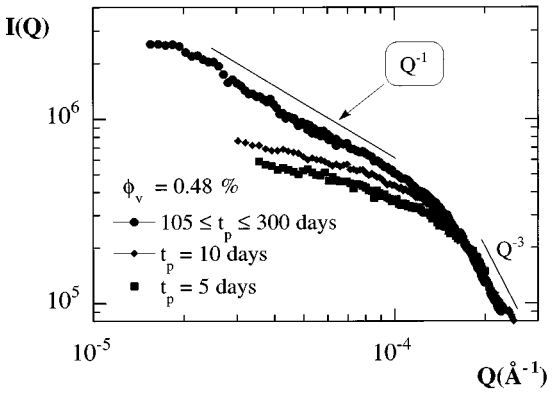

FIG. 8. Static light scattering from Laponite suspensions at different equilibrium gelation times (t_p), at 0.48% volume fraction, $I_s=1\times10^{-3}M$, and pH=9.5.

eliminated by electrostatic repulsions. If the depression extends from Q_1 to Q_2, this means that the dispersion appears, on average, homogeneous over scales extending from $d=1/Q_2$ to $a=1/Q_1$. The shorter of these distances d is the longest distance between neighboring particles (below this distance the dispersion appears homogeneous). The larger one a is the size of the elementary heterogeneities such as regular stacks of particles (''subunits''). For instance, according to the depression seen in Fig. 6, in the dispersion made at volume fraction 1.2%, interparticle distances are below $d=70$ Å and the elementary dense regions (subunits) are above $a=350$ Å; between these two scales, the dispersion appears homogeneous.

The interparticle correlations are disrupted by the addition of salt. This is shown in Fig. 7, where the plateau of the intensity disappears when the ionic strength is raised from $5\times10^{-4}M$ to $5\times10^{-3}M$. Accordingly, the size of the subunits is reduced from 350 to 100 Å; in other words, the regular stacks of particles split into smaller ones.

C. Large-scale aggregation and mechanical properties

At larger scales (lower Q), the scattering curves indicate that the regular stacks of particles (subunits) are aggregated into larger objects. For all dispersions, there is a Q^{-3} slope, which indicates that the aggregates are dense at scales extending up to 1 μm. At still lower-Q values, the less steep slope observed in light scattering indicates that the very-large-scale aggregation (1–5 μm) is less dense. This slope varies with the time of equilibration, with the concentration of Laponite, and with the ionic strength; simultaneously, there is a variation in the mechanical properties of the samples. In this section we focus on these changes.

Changes with time and volume fraction are as follows (Figs. 8 and 9). At very short times the slope of the intensity is nearly flat in this range of Q values, indicating that the dense micrometer-sized aggregates have been dispersed at random by the mixing procedure. At longer times, the slope becomes steeper, indicating some further aggregation; simultaneously, the mechanical properties become those of a gel.

For the lowest volume fraction ($0.35\% \leqslant \phi_v \leqslant 0.48\%$, Fig. 8) this process is quite slow and after 100 days the slope appears to have stabilized; the saturation value of the exponent is -1, corresponding to aggregates that are very tenuous or even stringy. For the higher volume fractions ($0.6\% \leqslant \phi_v \leqslant 2\%$) (Fig. 9), the changes proceed more rapidly and after 300 days the exponent reaches -1.8, which is the usual exponent for cluster-cluster aggregation [19–21]. A picture of these aggregates is presented in Fig. 10.

There is also a significant effect of ionic strength on the measured exponents. Upon going from $5\times10^{-4}M$ to 5

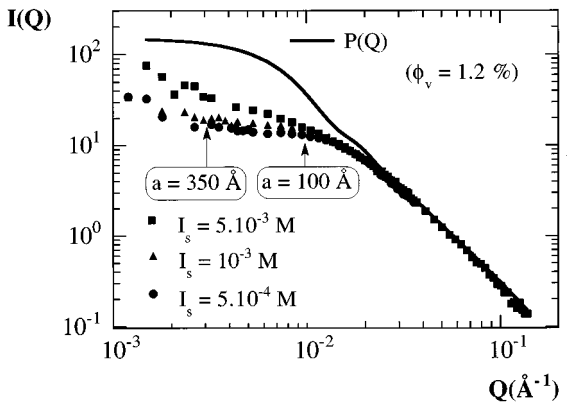

FIG. 7. Scattering intensity $I(Q)$ and form factor $P(Q)$ for Laponite suspensions at 1.2% volume fraction, at different ionic strengths, pH=9.5, and t_p=530 days.

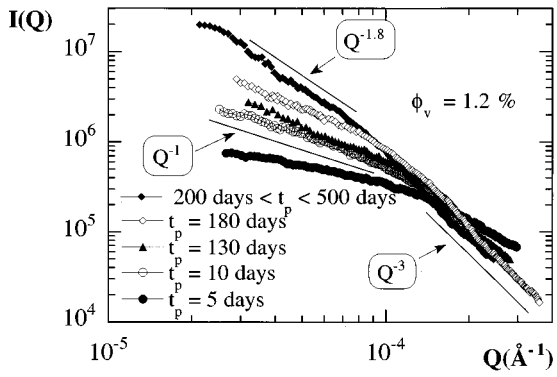

FIG. 9. Static light scattering from Laponite suspensions at different equilibrium gelation times (t_p), 1.2% volume fraction, $I_s=1\times10^{-3}M$, and pH=9.5.

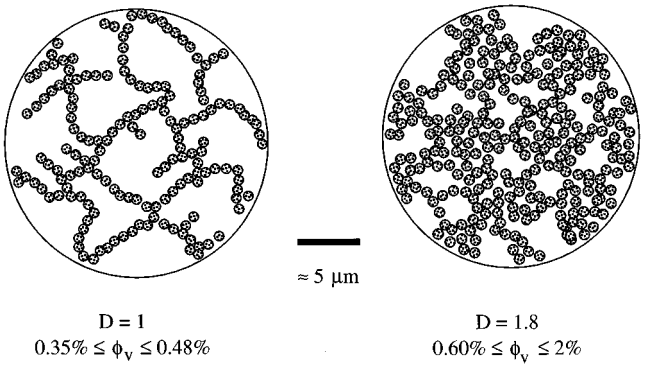

FIG. 10. Structure of Laponite suspensions according to volume fraction and fractal dimensions, $t_p \geqslant 300$ days.

$\times 10^{-3} M$ salt, the exponent changes from -1.6 to -2, indicating that the 5-μm aggregates become denser still [Fig. 11(a)]. The volume fraction dependence on the fractal dimension is shown in Fig. 12(a).

The corresponding changes in mechanical properties are presented in Figs. 11(b) and 12(b). In the viscoelastic linear regime ($\gamma = 0.05$ and $F = 0.1$ Hz), for buildup time greater than 1800 s, the mechanical response $G'(t), G''(t)$ becomes stiffer as the ionic strength is raised and the fractal dimension increases from 1.6 to 2 (Fig. 11). In the regime of permanent flow, the mechanical response is characterized by a yield stress [Fig. 12(b)]. This yield stress scales with the volume fraction of Laponite in the dispersion. At low volume fractions ($0.35\% \leqslant \phi_v \leqslant 0.48\%$) the exponent is 2. At high volume fractions ($0.6\% \leqslant \phi_v \leqslant 2\%$) it changes to 3. The change occurs simultaneously with the change in fractal dimensions. Thus aggregates with a higher fractal dimension give a higher elastic modulus and a yield stress that increases more rapidly with volume fraction.

A scaling law proposed by Dorget, Palierne, and Piau [14] for silica-silicon compounds in a domain of semidiluted fractal objects enables the fractal dimension measured by light scattering to be linked with the change in yield stress (measured by the vane method) as a function of volume fraction [14,15] [Fig. 12(b)]. The scaling law is defined as

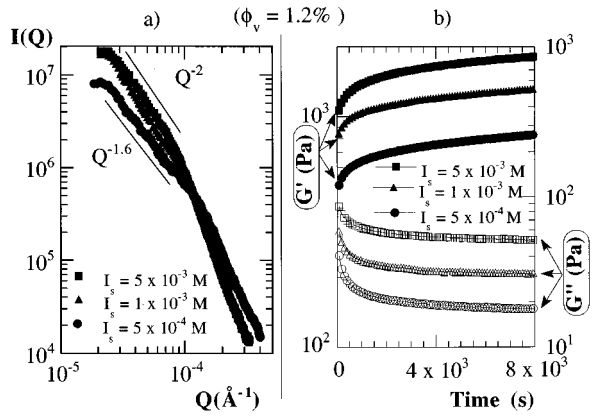

FIG. 11. (a) Static light scattering and (b) dynamic shear of Laponite suspensions, at small amplitude strain (0.05) at fixed frequency (0.1 Hz) at 1.2% volume fraction, different ionic strength I_s, pH = 9.5, and $t_p = 530$ days.

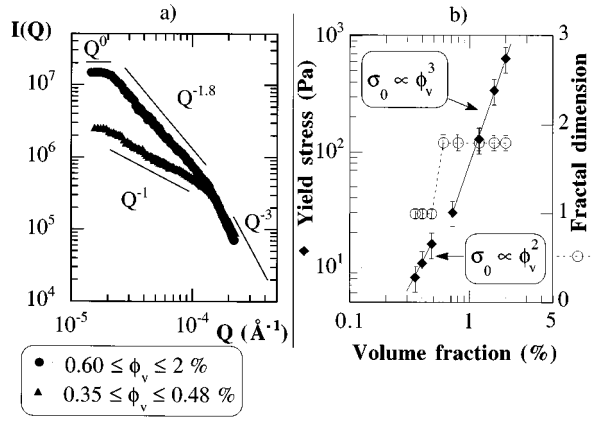

FIG. 12. (a) Static light scattering from Laponite suspensions at rest, at different volume fractions. (b) Change in yield stress at different volume fractions. $I_s = 1 \times 10^{-3} M$, pH = 9.5, and $t_p \geqslant 300$ days. With increasing volume fractions, the connection between micrometer-sized aggregates becomes tighter and tighter, giving rise to a more heterogeneous structure. The yield stress follows a power-law dependence on the volume fraction.

$$\sigma_0 \approx \beta \frac{kT}{a^3} \frac{R}{a} (\Phi_v)^{4/(3-D)},$$

in which σ_0 is the yield stress, ϕ_v is the particle volume fraction, D is the fractal dimension, and β takes into account the rigidity of the structure, as well as a volume fraction cofactor due to the inner density of subunits and, in an addition, an effective interaction much larger than kT. k is the Boltzmann constant, T the temperature, a the radius of a single particle (here a single subunit), and R the radius of gyration of the aggregates.

Good agreement was obtained between the rheometric measurements and predictions made with the scaling law associated with light-scattering measurements. With volume fractions close to the sol-gel transition, the fractal dimension is close to unity and the yield stress follows a $\phi_v^{2 \pm 0.3}$ power law. Beyond the critical volume fraction ϕ_{vc} of about 0.55%, the fractal dimension is 1.8 ± 0.1 and the yield stress follows a $\phi_v^{3 \pm 0.3}$ power law. Predictions using the scaling law give $\sigma_0 \propto \Phi_v^{2 \pm 0.05}$ and $\sigma_0 \propto \Phi_v^{3.3 \pm 0.3}$ behaviors for fractal dimensions of 1 ± 0.05 and 1.8 ± 0.1, respectively.

This correlation between fractal dimension and yield stress may be understood in the following way. The scattered intensity at $Q \rightarrow 0$ for samples with volume fractions exceeding critical ϕ_{vc} are five times larger than for samples with ϕ_v below critical ϕ_{vc}. This excess intensity shows that the structure of suspensions with volume fractions higher than $\phi_{vc} \approx 0.55\%$ is more heterogeneous, with areas of greater and lesser particle density.

It may be concluded that near a critical volume fraction, there is a change in structure from a homogeneous fibrous texture of micrometer-sized aggregates to a more heterogeneous network consisting of dense, micrometer-sized aggregates that are loosely interconnected, thus leaving areas of lower particle density (Fig. 10). From a macroscopic point of

view, this structural change near the critical volume fraction means that the yield stress is increasingly dependent on the volume fraction. The areas of high particle density appear to be responsible for this increasing dependence in yield stress at higher volume fractions.

The correlations that have been established between the fractal dimensions and rheological properties of this clay suspension should be compared with similar correlations observed with other colloidal suspensions. For example, mention may be made of the work of Axford and Herrington [18] on a natural Bentonite clay. These authors showed that the fractal dimension in this clay, determined by static light scattering, displays a rapid transition from a value $D=3$ below $p\mathrm{H}=4.3$ to a value $D=1.8$ above $p\mathrm{H}=4.3$. Rheometric measurements show a minimum yield stress at the point of intersection of $p\mathrm{H}=4.3$. Moreover, the ratio of G'/G'' has only two values: a high one below $p\mathrm{H}=4.3$ and a low one above $p\mathrm{H}=4.3$. The authors associate, respectively, a bandlike structure with tight connections and a more open house-of-cards-type structure to the fractal dimensions of 3 and 1.8. Rheometric measurements show that the aggregates of the closed structure ($D=3$) are more rigid that those of the open structure ($D=1.8$).

Shih *et al.* [23] have proposed a scaling theory connecting the viscoelastic properties of colloidal gels to the fractal dimension of the suspended objects. This law enabled them to show that variations in the elastic modulus G' and limit of linearity γ_c as a function of particle concentration are dictated by the fractal nature of the colloidal flocs. Rheometric and static light-scattering measurements on Boehmite alumina gels showed that these parameters had a power-law-type behavior in relation to the volume fraction. By applying the scaling law to analyze the rheometric data, they again found the fractal dimension determined by light scattering.

Finally, Dorget, Palierne, and Piau [14] carried out rheometric measurements on silica-silicon compounds and demonstrated that there was a power-law dependence of 3.3 for the yield stress and of 4.2 for the elastic modulus in relation to the volume fraction. These dependences were correctly described by a scaling law associated with light scattering to determine the fractal dimension $D=1.8$ of the objects forming the structure of their compounds.

The above examples and our measurements on Laponite suspensions concur in showing that the viscoelastic properties appear to be governed by the fractal dimension of the aggregates forming the structure. The fractal dimensions and hence the state of particle densification in the structural aggregates appear to be mainly responsible for the change in yield stress and viscoelastic moduli in relation to the physicochemical parameters (volume fraction, ionic strength, and $p\mathrm{H}$) of these colloidal suspensions. Furthermore, scaling laws associated with either scattering or rheometric measurements enable us to relate the structural information to the macroscopic properties of these colloidal systems.

IV. CONCLUSION

This study identified characteristic length scales of the structure of a colloidal suspension of synthetic clay. The network that is created as the suspension swells, leading to the formation of a thixotropic gel, is due to the formation of micrometer-sized aggregates. Combining in loose associations, the micrometer-sized aggregates form a continuous, three-dimensional isotropic structure. Below a critical volume fraction, these aggregates form bundles that give Laponite suspensions a fibrous texture. Beyond the critical volume fraction, the structure is more heterogeneous, with areas of varying particle density.

This influence of the volume fraction on the structure was correlated with the yield stress of these suspensions by means of a scaling law. It appears that the fractal dimension, and hence the degree of particle densification in the aggregates, governs the change in yield stress with volume fraction. The study of the influence of ionic strength and equilibrium gelation time on the structure of the suspensions showed that changes in fractal dimensions govern the elastic modulus and yield stress values and hence the mechanical behavior.

This work stresses the following point: It is necessary to conduct a careful analysis of the structure of concentrated colloidal suspensions over a wide range of length scales in order to understand their rheological behavior. The correlations established between the fractal dimensions and rheological properties of this clay suspension should be compared with correlations of the same type made with other colloidal suspensions. Examples worthy of mention include the natural Bentonite clay suspensions studied by Axford and Herrington [18], Boehmite alumina gels [23], and silica-silicon compounds [14]. All these correlations suggest that both the scales of the largest structure (in our case the pertinent length scale of the order of 1 μm) and the fractal dimensions of the aggregates are mainly responsible for the rheological behaviors observed in these types of colloidal suspensions.

[1] J. D. F. Ramsay, S. W. Swanton, and J. Bunce, J. Chem. Soc. Faraday Trans. **86**, 3919 (1990).

[2] H. Van Olphen, *An Introduction to Clay Colloid Chemistry* (Wiley, New York, 1977).

[3] N. C. Lockhart, J. Colloid Interface Sci. **74**, 509 (1980).

[4] J. Fripiat, J. Cases, M. Francois, and M. Letellier, J. Colloid Interface Sci. **89**, 378 (1982).

[5] L. Rosta and H. R. Von Gunten, J. Colloid Interface Sci. **134**, 397 (1990).

[6] J. D. F. Ramsay and P. Lindner, J. Chem. Soc. Faraday Trans. **89**, 4207 (1993).

[7] M. Morvan, D. Espinat, J. Lambard, and Th. Zemb, Colloids Surf., A **82**, 193 (1994).

[8] A. Mourchid, A. Delville, J. Lambard, E. Lécolier, and P. Lev-

itz, Langmuir **11**, 1942 (1995).
[9] F. Pignon, A. Magnin, and J. M. Piau, J. Rheol. **40**, 573 (1996).
[10] D. W. Thomson and J. T. Butterworth, J. Colloid Interface Sci. **151**, 236 (1992).
[11] P. Bösecke, O. Diat, and B. Rasmussen, Rev. Sci. Instrum. **66**, 1636 (1995).
[12] O. Diat, P. Bösecke, and J. Gorini, Cahiers Rhéol. **13**, 81 (1994).
[13] P. Lindner and R. C. Oberthür, Rev. Phys. Appl. **19**, 759 (1984).
[14] M. Dorget, Ph.D. thesis, Institute National Polytechnique at Grenoble 1995 (unpublished); M. Dorget, J. F. Palierne, and J. M. Piau (unpublished).
[15] F. Pignon, J. M. Piau, and A. Magnin, Phys. Rev. Lett. **76**, 4857 (1996).
[16] A. Magnin and J. M. Piau, J. Non-Newtonian Fluid Mech. **36**, 85 (1990).
[17] N. Willenbacher, J. Colloid Interface Sci. **182**, 501 (1996).
[18] S. D. T. Axford and T. M. Herrington, J. Chem. Soc. Faraday Trans. **90**, 2085 (1994).
[19] P. Meakin, Phys. Rev. A **27**, 604 (1983).
[20] P. Meakin, Phys. Rev. Lett. **51**, 1119 (1983).
[21] M. Kolb, R. Botet, and R. Jullien, Phys. Rev. Lett. **51**, 1123 (1983).
[22] A. Guiner and G. Fournet, *Small Angle Scattering of X-Rays* (Wiley, New York, 1955).
[23] W. H. Shih, W. Y. Shih, S. I. Kim, J. Liu, and I. A. Aksay, Phys. Rev. A **42**, 4772 (1990).